

# PPAR $\gamma$ /RXR $\alpha$ -Induced and CD36-Mediated Microglial Amyloid- $\beta$ Phagocytosis Results in Cognitive Improvement in Amyloid Precursor Protein/Presenilin 1 Mice

Mitsugu Yamanaka,<sup>1,2</sup> Taizo Ishikawa,<sup>1,2</sup> Angelika Griep,<sup>1</sup> Daisy Axt,<sup>1</sup> Markus P. Kummer,<sup>1</sup> and Michael T. Heneka<sup>1,3</sup>

<sup>1</sup>Clinical Neuroscience Unit, Department of Neurology, University of Bonn Medical Center, 53127 Bonn, Germany, <sup>2</sup>Dainippon Sumitomo Pharma, 564-0053 Osaka, Japan, and <sup>3</sup>German Center for Neurodegenerative Diseases, 53127 Bonn, Germany

Alzheimer's disease (AD) is characterized by the extracellular deposition of amyloid- $\beta$  (A $\beta$ ), neurofibrillary tangle formation, and a microglial-driven inflammatory response. Chronic inflammatory activation compromises microglial clearance functions. Because peroxisome proliferator-activated receptor  $\gamma$  (PPAR $\gamma$ ) agonists suppress inflammatory gene expression, we tested whether activation of PPAR $\gamma$  would also result in improved microglial A $\beta$  phagocytosis. The PPAR $\gamma$  agonist pioglitazone and a novel selective PPAR $\alpha/\gamma$  modulator, DSP-8658, currently in clinical development for the treatment of type 2 diabetes, enhanced the microglial uptake of A $\beta$  in a PPAR $\gamma$ -dependent manner. This PPAR $\gamma$ -stimulated increase of A $\beta$  phagocytosis was mediated by the upregulation of scavenger receptor CD36 expression. In addition, combined treatment with agonists for the heterodimeric binding partners of PPAR $\gamma$ , the retinoid X receptors (RXRs), showed additive enhancement of the A $\beta$  uptake that was mediated by RXR $\alpha$  activation. Evaluation of DSP-8658 in the amyloid precursor protein/presenilin 1 mouse model confirmed an increased microglial A $\beta$  phagocytosis *in vivo*, which subsequently resulted in a reduction of cortical and hippocampal A $\beta$  levels. Furthermore, DSP-8658-treated mice showed improved spatial memory performance. Therefore, stimulation of microglial clearance by simultaneous activation of the PPAR $\gamma$ /RXR $\alpha$  heterodimer may prove beneficial in prevention of AD.

## Introduction

Cerebral inflammation occurs through the activation of microglia, the brain innate immune system in response to misfolded or aggregated proteins and neuronal debris. In addition to its classical hallmarks, amyloid- $\beta$  (A $\beta$ ) deposition and neurofibrillary tangle formation, Alzheimer's disease (AD) is characterized by a neuroinflammatory component (Lucin and Wyss-Coray, 2009). In AD, activated microglia are found in close vicinity to A $\beta$  deposits and produce a wide range of cytokines and chemokines (Rogers and Lue, 2001). Because microglia are critical for A $\beta$  phagocytosis, the microglial presence at the A $\beta$  plaque can be interpreted as an attempt to clear this pathological deposit. Evidence for an important role of microglial phagocytosis comes from studies that show that restricting microglial A $\beta$  uptake leads to increased cerebral A $\beta$  levels (El Khoury et al., 2007; Lee and Landreth, 2010). Microglial expression of receptors that promote the clearance and phagocytosis of A $\beta$ , such as CD36, TLR4, and

TLR6 (Lee and Landreth, 2010), are mandatory for restricting amyloid plaque formation. However, as AD progresses, microglia acquire a chronically activated phenotype through unremitting stimulation by cytokines and A $\beta$  itself, which compromises their clearance function (Bamberger et al., 2003; Hickman et al., 2008; Heneka et al., 2010a).

Because impaired A $\beta$  clearance is likely to account for the majority of sporadic AD cases (Mawuenyega et al., 2010), identification of factors that regulate microglial A $\beta$  uptake seems to be of utmost importance.

The recognition that a robust inflammatory response contributes to AD also fuelled the discovery that long-term treatment with non-steroidal anti-inflammatory drugs (NSAIDs) reduced the risk for AD, delayed disease onset, and slowed cognitive decline (McGeer et al., 1996; Stewart et al., 1997; in t' in t'Veld et al., 2001). Of note, a subset of NSAIDs directly regulates gene expression through binding and activating the peroxisome proliferator-activated receptor- $\gamma$  (PPAR $\gamma$ ) (Lehmann et al., 1997) that belongs to the nuclear receptor superfamily and forms a heterodimer with the retinoid X receptor (RXR) before binding to PPAR response elements in the promoter region of target genes. Currently marketed PPAR $\gamma$  ligands modulate insulin sensitivity but also cause considerable side effects, including body weight gain and fluid retention. DSP-8658 is a novel selective PPAR $\alpha/\gamma$  modulator that is currently developed for type 2 diabetes, because the described side effects are absent in relevant preclinical models.

In microglia and macrophages, PPAR $\gamma$  activation inhibits proinflammatory gene expression (Jiang et al., 1998; Ricote et al.,

Received March 29, 2012; revised Aug. 31, 2012; accepted Sept. 27, 2012.

Author contributions: M.Y., M.P.K., and M.T.H. designed research; M.Y., T.I., A.G., D.A., and M.P.K. performed research; M.Y. contributed unpublished reagents/analytic tools; M.Y., M.P.K., and M.T.H. analyzed data; M.Y. and M.T.H. wrote the paper.

This research was supported in part by a grant from Dainippon Sumitomo Pharma and German Research Foundation Grant KFO177 (M.T.H.). We are grateful to Drs. C. Pietrzik and S. Weggen for providing antibody IC16.

This article is freely available online through the *JNeurosci* Open Choice option.

Correspondence should be addressed to Dr. Michael T. Heneka, Department of Neurology, University of Bonn, Sigmund Freud Strasse 25, 53127 Bonn, Germany. E-mail: michael.heneka@ukb.uni-bonn.de.

DOI:10.1523/JNEUROSCI.1569-12.2012

Copyright © 2012 the authors 0270-6474/12/3217321-11\$15.00/0

1998). In the brain, PPAR $\gamma$  agonists reduce A $\beta$ - and cytokine-mediated neuroinflammation and neurotoxicity *in vitro* (Heneka et al., 1999; Combs et al., 2000) and *in vivo* (for review, see Heneka and Landreth, 2007).

Here we demonstrate the potential of the PPAR $\gamma$  ligand pioglitazone and the PPAR $\alpha$ / $\gamma$  modulator DSP-8658 to modulate microglial A $\beta$  phagocytosis *in vitro* and *in vivo*.

## Materials and Methods

**Materials.** DSP-8658 was provided from Dainippon Sumitomo Pharma. Pioglitazone was obtained by Takeda Pharmaceuticals. 9-*cis*-Retinoic acid, actinomycin D, and cycloheximide were obtained from Sigma-Aldrich. Bexarotene was purchased from LC Laboratories. Rat PPAR $\gamma$  siRNA (L-080081-01-0010), rat RXR $\alpha$  siRNA (L-089934-01-0010), rat RXR $\beta$  siRNA (L-094287-01-0010), and nontargeting control siRNA (D-001810-10-05) were purchased from Thermo Fisher Scientific.

**Primary microglial cell culture.** Primary microglial cell cultures were prepared as described previously in detail (Terwel et al., 2011). Briefly, mixed glial cultures were prepared from newborn rat or mouse cultured in DMEM supplemented with 10% FCS and 100 U/ml penicillin/streptomycin. Microglial cells were used after 10–14 d of primary cultivation. They were harvested by shake off, seeded, and allowed to attach to the substrate for 30–60 min.

**Transactivation assay.** Monkey kidney COS-1 cells were maintained in standard culture conditions (DMEM) supplemented with 10% FCS, 1% sodium pyruvate, 1% essential amino acids, and 1% streptomycin/penicillin at 37°C in a humidified atmosphere of 5% CO<sub>2</sub>. The medium was changed every other day. Cells were transfected with GAL4-UAS-luc plasmid and the plasmid coding the nuclear receptor of interest (GAL4 DNA-BD/PPAR $\alpha$ -LBD, GAL4 DNA-BD/PPAR $\gamma$ -LBD). Transfected cells were incubated for 24 h at 37°C in medium containing the compound tested. The luciferase activity was measured with the Steady-Glo Luciferase Assay System (Promega). The reference compounds for PPAR $\alpha$  and PPAR $\gamma$  were fenofibrate and rosiglitazone, respectively.

**Phagocytosis of 6-carboxyfluorescein-labeled A $\beta$ <sub>1–42</sub> by microglia.** Microglial phagocytosis of 6-carboxyfluorescein (FAM)-labeled A $\beta$ <sub>1–42</sub> (FAM-A $\beta$ ) (Peptide Specialty Laboratories) was measured by plate-based assay as described previously (Floden and Combs, 2006). In brief, cells were plated at a density of 50,000 per well. Cells were incubated with 500 nM A $\beta$  for up to 4 h, starting 1 h after plating. The A $\beta$ -containing medium was removed, and extracellular A $\beta$  was quenched with 100  $\mu$ l of 0.2% trypan blue in PBS, pH 4.4, for 1 min. After aspiration, fluorescence was measured at 485 nm excitation/535 nm emission using an Infinity 200 reader (Tecan). To normalize for cell numbers, cells were incubated with 100  $\mu$ l of 50  $\mu$ g/ml H33342 [2'-(4-ethoxyphenyl)-5-(4-methyl-1-piperazinyl)-2,5'-bi-1H-benzimidazole trihydrochloride] in PBS and 0.1% Triton X-100 for 15 min, and fluorescence was measured at 360 nm excitation/465 nm emis-

**Table 1. Activation of human PPARs by DSP-8658**

Compound	Human, EC <sub>50</sub>	
	$\alpha$	$\gamma$
DSP-8658	1.08 $\mu$ M	1.01 $\mu$ M (76%)
Pioglitazone	>10 $\mu$ M	0.52 $\mu$ M (100%)
Rosiglitazone		0.084 $\mu$ M (104%)
Fenofibric acid	16.9 $\mu$ M	

Activation of PPAR $\alpha$  and PPAR $\gamma$  was determined by transactivation assay in COS-1 cells after incubation with compounds for 24 h. The reference compounds for PPAR $\alpha$  and PPAR $\gamma$  were fenofibrate and rosiglitazone, respectively.

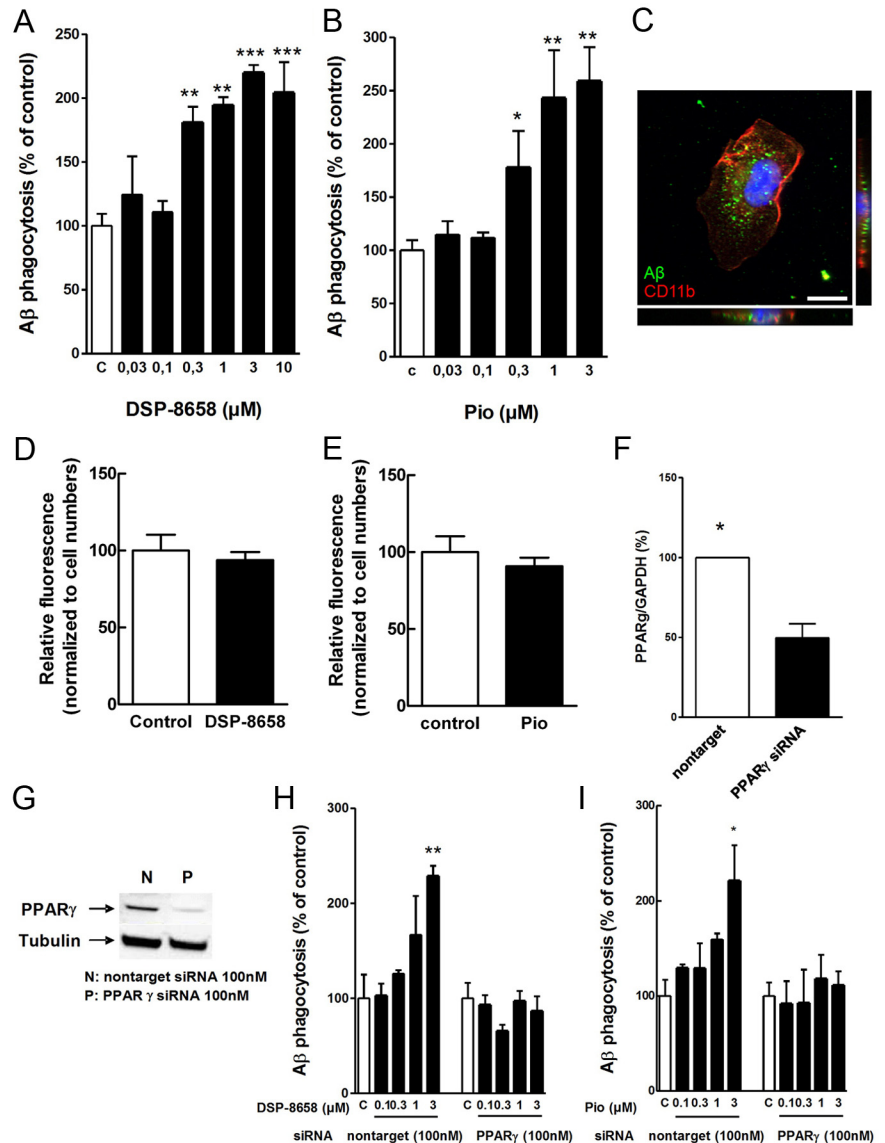


**Figure 1.** Effect of PPAR $\gamma$  agonist on A $\beta$  phagocytosis in primary microglia. Rat primary microglia were incubated with increasing concentrations of DSP-8658 or pioglitazone in the presence of FAM-A $\beta$  (0.5  $\mu$ M). After 4 h exposure to A $\beta$ , intracellular levels of A $\beta$  were determined. Both DSP-8658 (**A**) and pioglitazone (**B**) enhanced the uptake of A $\beta$  in rat primary microglia in a concentration-dependent manner (mean  $\pm$  SEM of  $n = 3$ , \* $p < 0.05$ , \*\* $p < 0.01$ , \*\*\* $p < 0.001$ , one-way ANOVA, Tukey's *post hoc* test). **C**, Intracellular uptake of A $\beta$ <sub>1–42</sub> was confirmed by immunocytochemical staining of A $\beta$  using antibody IC16 and the cell-surface antigen CD11b using antibody MCA711. Scale bar, 10  $\mu$ m. Rat primary microglia were incubated for 30 min with FAM-A $\beta$  in the presence of 0.3  $\mu$ M DSP-8658 (**D**) or 0.3  $\mu$ M pioglitazone (pio) (**E**) (mean  $\pm$  SEM of  $n = 3$ ). PPAR $\gamma$  mRNA (**F**) and protein levels (**G**) in primary microglia transfected with siRNA for PPAR $\gamma$  (mean  $\pm$  SEM of  $n = 3$ , \* $p < 0.05$ , Student's *t* test). Primary microglia transfected with siRNA for PPAR $\gamma$  or nontarget were incubated with DSP-8658 (**H**) or pioglitazone (**I**) in the presence of FAM-A $\beta$  (0.5  $\mu$ M). DSP-8658 and pioglitazone enhanced A $\beta$  uptake at 3  $\mu$ M in nontarget control siRNA-treated primary microglia, although the same treatments failed to increase A $\beta$  phagocytosis in PPAR $\gamma$  siRNA-treated primary microglia (mean  $\pm$  SEM of  $n = 3$ , \* $p < 0.05$ , \*\* $p < 0.01$ , one-way ANOVA, Tukey's *post hoc* test).

sion. For analysis of intracellular A $\beta$  degradation, cells were incubated for 30 min with pioglitazone or DSP-8658. Afterward, FAM-A $\beta$ <sub>1–42</sub> was added for 30 min, and the cell culture media were replaced. After 4 h of incubation, fluorescence was determined as described above. For intracellular localization of A $\beta$  mouse primary microglia, cells were incubated with 150 nM A $\beta$ <sub>1–42</sub>. Cells were fixed in 4% paraformaldehyde, permeabilized with 0.1% Triton X-100 in PBS, and blocked with 20% goat serum in PBS. Subsequently, cells were coincubated with antibodies IC16 against A $\beta$  (Jäger et al., 2009) and MCA711 (AbD Serotec) against CD11b. Fluorescence microscopy was done on an BX61 equipped with a disc-spinning unit (Olympus). Microglial cell death in response to drug or A $\beta$  exposure was excluded by LDH assay.

**Nucleofection of siRNA.** All electroporations were performed using Nucleofector II (Lonza) and the mouse macrophage nucleofection kit (Amaxa Biosystems) according to the instructions of the manufacturer.

**Western blotting.** Protein concentration in the RIPA-soluble or SDS-soluble fraction was determined using the BCA Protein Assay kit (Pierce). Protein samples (10–50  $\mu$ g) were separated by 4–12% NuPAGE (Invitrogen) using MES buffer and transferred to nitrocellulose membranes. Protein levels of PPAR $\gamma$  [anti-PPAR $\gamma$  (H-100); Santa Cruz Biotechnology], RXR $\alpha$  [anti-RXR $\alpha$  (PP-K8508); Perseus Proteomics], RXR $\beta$  [anti-RXR $\beta$  (PP-H7341); Perseus Proteomics] (1:500), CD36 [anti-CD36 (ab36977); Abcam], and tubulin [E7; Developmental Studies Hybridoma Bank] were assessed. Primary antibody incubation was followed by incubation with appropriate horseradish peroxidase-conjugated secondary antibodies. Immunoreactivity was detected by enhanced chemiluminescence reaction (Millipore), and luminescence intensities were analyzed using Chemidoc XRS documentation system (Bio-Rad).

**RNA preparation and real-time reverse transcription-polymerase chain reaction.** Total RNA was isolated from microglia using the RNeasy Mini kit (Qiagen) and quantified spectrophotometrically and reverse transcribed using the RevertAid First Strand cDNA Synthesis kit (Fermentas) according to the instructions of the manufacturer. Predesigned PPAR $\gamma$ , CD36, and GAPDH primers were purchased from Applied Biosystems. The real-time PCR reactions were performed using the StepOnePlus PCR System (Applied Biosystems). mRNA expression values were normalized to the level of GAPDH expression.

**Animals.** Amyloid precursor protein/presenilin 1 (APP/PS1) transgenic animals expressing the mouse APP containing the human A $\beta$  domain as well as the Swedish mutation and the PS1  $\Delta$ exon 9 mutation both under the control of the prion promoter were used (Jankowsky et al., 2001). Three-month-old wild-type and APP/PS1 transgenic mice were divided into control and DSP-8658-treated groups and fed with a standard food not containing substance or containing 0.1% DSP-8658 for 3 months. The amounts of food and body weight were assessed weekly. The daily food intake was calculated from the following equation: daily food intake (g/d) = total food intake during the treatment period/treatment days. The mean dose administered to the DSP-8658-treated group was estimated from the following equation: estimated administered dose (mg  $\cdot$  kg<sup>-1</sup>  $\cdot$  d<sup>-1</sup>) = daily food intake  $\times$  1000  $\times$  0.1% (content of DSP-8658 in the diet)/100/mean body weight during the dosing period. Mice were housed in groups under standard conditions at a temperature of 22  $\pm$  1°C and a 12 h light/dark cycle with access to standard food (Altromin) and water *ad libitum*. Animal care and handling were performed according to the Declaration of Helsinki and approved by local ethical committees. Mice were deeply anesthetized with isoflurane and killed, and brains were removed and processed for neurochemical and immunochemical determinations.

**Morris water maze.** The test was conducted in a pool consisting of a circular tank (1 m diameter) filled with opacified water at 24°C. The water basin was dimly lit (20–30 lux) and surrounded by a white curtain. The maze was virtually divided into four segments (quadrants). In one of the quadrants, a hidden platform (15  $\times$  15 cm) was present 1.5 cm below the water surface. Mice were trained to find the platform, orientating by means of three intermaze cues placed asymmetrically as spatial references. They were let into the water in a quasi-random manner to prevent strategy learning. Mice were allowed to search for the platform for 40 s. If the mice did not reach the platform in the allotted time, they

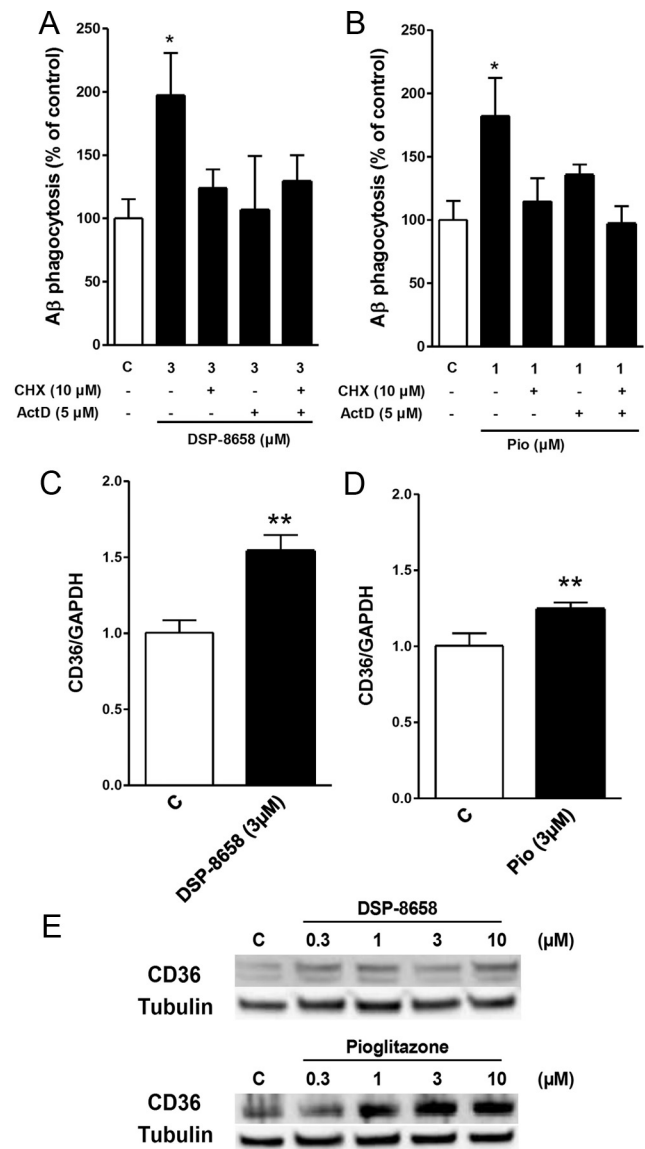


**Figure 2.** Effects of PPAR $\gamma$  agonist on CD36 expression in primary microglia. Primary microglia was coincubated with inhibitors of transcription [actinomycin D (ActD), 5  $\mu$ M] or translation [cycloheximide (CHX), 10  $\mu$ M] in the presence of FAM-A $\beta$  (0.5  $\mu$ M). After 4 h, intracellular levels of A $\beta$  were determined. A $\beta$  phagocytosis by DSP-8658 (**A**) or pioglitazone (**B**) was abolished by coincubation with the respective inhibitors. The data show the intracellular A $\beta$  uptake as percentage of control (mean  $\pm$  SEM of  $n = 3$ , \* $p < 0.05$ , one-way ANOVA, Tukey's *post hoc* test). **C–E**, Primary microglia was incubated with DSP-8658 or pioglitazone for 6 h, and CD36 mRNA and protein levels were detected. CD36 mRNA was upregulated in response to DSP-8658 (**C**) or pioglitazone (**D**), followed by an increase of the respective protein levels in a concentration-dependent manner (**E**) (mean  $\pm$  SEM of  $n = 3$ , \*\* $p < 0.01$ , Student's *t* test).

were placed manually on it. The mice were allowed to stay on the platform for 15 s before the next trial was started. After four trials were completed, mice were dried and placed back in their home cage. Mice received four training trials per day for 8 consecutive days. Movements of the mice were recorded by a computerized tracking system that calculated distances moved and latencies (Noldus).

**Extraction of brain lysates.** Snap-frozen forebrain hemispheres were homogenized in PBS with protease inhibitor mixture (Sigma). Protein was extracted in RIPA (25 mM Tris-HCl, pH 7.5, 150 mM NaCl, 0.5% sodium desoxycholate, 1% NP-40, and 0.1% SDS) for 30 min on ice. After centrifugation at 100,000  $\times$   $g$  for 30 min at 4°C, the resulting supernatant (RIPA-soluble fraction) was saved, and the pellet was sonified in 25 mM Tris-HCl, pH 7.5, and 2% SDS (RIPA-insoluble fraction).

**A $\beta$  determination by sandwich ELISA.** Human (6E10) A $\beta_{1-40}$  or A $\beta_{1-42}$  ultrasensitive kits were used (Meso Scale Discovery). Signals were measured on a SECTOR Imager 2400 reader (Meso Scale Discovery).

**In vivo phagocytosis assay.** Six-month-old wild-type and APP/PS1 transgenic mice were intraperitoneally injected 3 h before the animals were killed with 10 mg/kg methoxy-X04 (kindly provided by Dr. Alfons Verbruggen, Catholic University of Leuven, Leuven, Belgium) in 50% DMSO/50% NaCl (0.9%), pH 12 (Bolmont et al., 2008). Mice were perfused with ice-cold PBS, the brain was removed, and one hemisphere was chopped into pieces using scalpels. Brain pieces were homogenized in HBSS, 0.6% glucose, and 15 mM HEPES, pH 7, using a Potter-Elvehjem tissue homogenizer. Additional homogenization was achieved by gently up and down pipetting using Pasteur pipettes with decreasing opening diameter. The resulting homogenate was filtered through a cell strainer (70  $\mu$ m) and centrifuged at 155  $\times$  g (Beckman Allegra) at 4°C for 10 min without brake. The pellet was resuspended in 9 ml of 75% Percoll in PBS and underlayered with ice-cold 10 ml of 25% Percoll in PBS and overlaid with 6 ml ice-cold PBS. The gradient was centrifuged at 800  $\times$  g at 4°C for 25 min (Beckman Allegra) without brake. Microglial cells are recovered from the 25/75% Percoll interphase, diluted with 3 vol of PBS, and centrifuged at 880  $\times$  g at 4°C for 25 min (Beckman Allegra) without brake. The pellet containing the microglial cells was resuspended in 200  $\mu$ l of PBS.

**Flow cytometry analysis of methoxy-X04 containing microglia.** Binding of antibodies to Fc receptors was prevented by adding Fc block (Merck) diluted 1:100 for 10 min on ice. Fifty microliters of cells were diluted with 0.5 ml of HBSS and centrifuged at 1000 rpm for 5 min at 4°C. Cells were taken up in 50  $\mu$ l of HBSS containing biotinylated TLR4 antibody (1:100), incubated 30 min on ice, and centrifuged at 1000 rpm for 5 min at 4°C. Cells were taken up in 50  $\mu$ l of HBSS containing streptomycin–phycoerythrin (PE)–Cy7 (1:200), incubated 30 min on ice, and centrifuged at 1000 rpm for 5 min at 4°C. Finally, cells were incubated with antibody mix [CD11b–adenomatous polyposis coli (APC), 1:100; CD45–FITC, 1:100] and incubated for 30 min on ice. Cells were centrifuged at 1000 rpm for 5 min at 4°C and resuspended in 200  $\mu$ l of HBSS. For control and compensation, we used corresponding isotype control antibodies. Samples were analyzed on an FACS Canto II flow cytometer (BD Bioscience). Data evaluation of the CD11b–positive (CD11b<sup>+</sup>)/CD45<sup>+</sup> population concerning methoxy-X04 incorporation was performed. Flow cytometry analysis of microglia was performed using antibodies CD11b–APC (catalog #101212; BioLegend), CD45–FITC (catalog #11-0451; eBioscience), and CD36–PE (catalog #12-0361; eBioscience).

**Immunohistochemistry.** Free-floating 40- $\mu$ m-thick serial sections were cut on a vibratome (Leica). Sections obtained were stored in 0.1% NaN<sub>3</sub> and PBS in a cold room. For immunohistochemistry, sections were treated with 50% methanol for 15 min. Then, sections were washed three times for 5 min in PBS and blocked in 3% BSA, 0.1% Triton X-100, and PBS (blocking buffer) for 30 min, followed by overnight incubation with

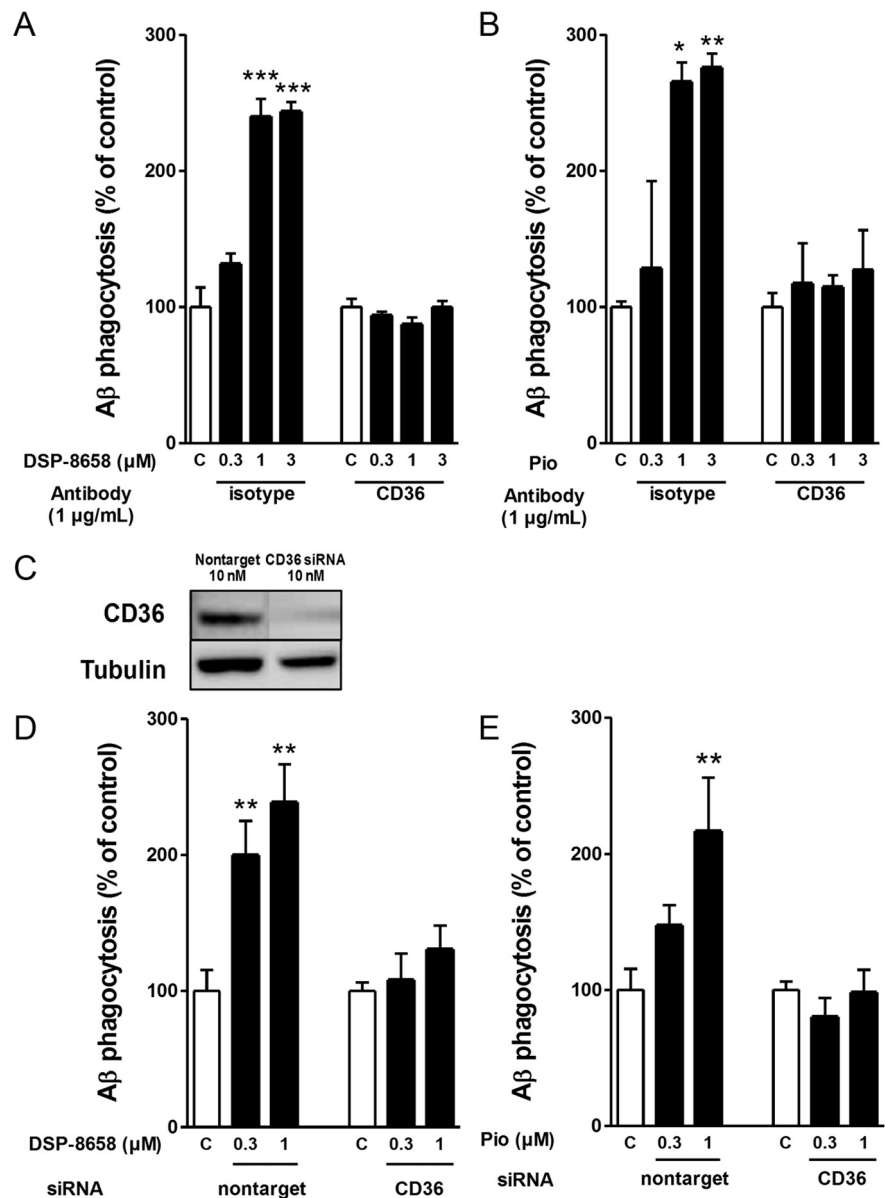


**Figure 3.** CD36 mediates the PPAR $\gamma$ -stimulated increase in microglial A $\beta$  uptake. Primary microglia was incubated for 4 h with either DSP-8658 (**A**) or pioglitazone (**B**; Pio) in the presence of CD36 antibody or isotype control. After 4 h, intracellular A $\beta$  was determined. PPAR $\gamma$  agonist-stimulated A $\beta$  phagocytosis was suppressed by coinubation with CD36 antibody (mean  $\pm$  SEM of  $n = 3$ , \* $p < 0.05$ , \*\* $p < 0.01$ , \*\*\* $p < 0.001$ , one-way ANOVA, Tukey's *post hoc* test). **C**, Protein levels of CD36 in primary microglia transfected with siRNA for CD36. **D, E**, Primary microglia transfected with siRNA for CD36 or nontarget were incubated with DSP-8658 or pioglitazone in the presence of FAM-labeled A $\beta_{1-42}$  (0.5  $\mu$ M). After 4 h, intracellular level of A $\beta$  was determined. Transfection of cell with CD36 siRNA blocked the PPAR $\gamma$  agonist-stimulated uptake of A $\beta$ . The data show the intracellular A $\beta$  uptake as percentage of control (mean  $\pm$  SEM of  $n = 3$ , \*\*\* $p < 0.01$ , one-way ANOVA, Tukey's *post hoc* test).

the primary antibody in blocking buffer. Next, sections were washed three times in 0.1% Triton X-100 and PBS and incubated with Alexa Fluor 488-conjugated or Alexa Fluor 594-conjugated secondary antibodies (1:500; Invitrogen) for 90 min, washed three times with 0.1% Triton X-100 and PBS for 5 min. Finally, the sections were mounted on glasses in tap water and embedded. The following primary antibodies were used with respective concentrations: rabbit polyclonal 2964 against A $\beta$  (1:400, generous gift from Dr. Jochen Walter) and rat monoclonal anti-mouse CD11b (1:200, Serotec). In thioflavin S staining, slices were rinsed in water, incubated in 0.01% thioflavin S in 50% ethanol, and differentiated in 50% ethanol. Fluorescence microscopy was done on an BX61 equipped with a disc-spinning unit (Olympus) or an A1-MP (Nikon) laser-scanning microscope, and images were processed in Cell-P (Olympus) or NIS elements (Nikon).

**Statistical analyses.** Data were analyzed by using Student's *t* test, one-way ANOVA followed by Tukey's *post hoc* test, or Dunnett's multiple comparison test using Prism 5.03 (GraphPad Software).

## Results

### Effects of PPAR $\gamma$ agonist on A $\beta$ phagocytosis in rat primary microglia

To test whether PPAR $\gamma$  agonists affect A $\beta$  phagocytosis, rat primary microglia were incubated with increasing concentrations of DSP-8658, a PPAR $\alpha/\gamma$  agonist with an EC<sub>50</sub> of  $\sim 1$   $\mu$ M for both isoforms (Table 1), or pioglitazone in the presence of FAM-A $\beta$  (0.5  $\mu$ M). After 4 h exposure to A $\beta$ , intracellular levels of A $\beta$  were determined. Both DSP-8658 and pioglitazone enhanced the uptake of A $\beta$  in rat primary microglia in a concentration-dependent manner (Fig. 1*A, B*). Intracellular presence of A $\beta$  in primary microglia was confirmed by immunocytochemistry using antibody IC16 against A $\beta$  and antibody MCA711 against the cell-surface antigen CD11b (Fig. 1*C*). Time-dependent intracellular degradation was analyzed as described previously (Fleisher-Berkovich et al., 2010) over the time course of 4 h and found to be similar between substances (Fig. 1*D, E*). Therefore, these results indicate that DSP-8658 and pioglitazone induce the phagocytic uptake of A $\beta$  by microglia. To firmly establish the contribution of PPAR $\gamma$  in the regulation of A $\beta$  phagocytosis and to exclude off-target drug effects, PPAR $\gamma$  gene expression was silenced by siRNA. Quantitative PCR analysis indicated that the siRNA transfection suppressed PPAR $\gamma$  gene expression by 50% (Fig. 1*F*), resulting in a substantial reduction of PPAR $\gamma$  protein levels when compared with the nontarget control siRNA (Fig. 1*G*). Although DSP-8658 and pioglitazone enhanced A $\beta$  uptake at 3  $\mu$ M in nontarget control siRNA-transfected primary microglia, the same treatments failed to increase A $\beta$  phagocytosis in PPAR $\gamma$  siRNA-transfected primary microglia (Fig. 1*H, I*). Comparing these results with Figure 1, *A* and *B*, it seemed that the phagocytic response during drug stimulation was reduced in the siRNA transfection experiments. Although cell death was excluded as the source of this phenomenon, siRNA transfection may have led to microglial prestimulation, resulting in an overall decreased phagocytic response. Together, these results suggest that microglial A $\beta$  clearance can be increased by PPAR $\gamma$  activation.

### Effects of PPAR $\gamma$ agonist on CD36 expression in primary microglia

To determine whether PPAR $\gamma$ -mediated A $\beta$  uptake requires *de novo* synthesis of mRNA and protein, rat primary microglia were coincubated with inhibitors of transcription (actinomycin D, 5  $\mu$ M) or translation (cycloheximide, 10  $\mu$ M). Interestingly, the increasing effect of DSP-8658 and pioglitazone was abolished once either actinomycin D or cycloheximide were coincubated, suggesting that *de novo* mRNA/protein synthesis is required (Fig. 2*A, B*).

To further address the mechanism underlying the stimulation of microglial A $\beta$  phagocytosis by PPAR $\gamma$  agonists, we focused on the search for a cell-surface marker that is regulated by PPAR $\gamma$  and is involved in A $\beta$  phagocytosis. Indeed, the expression of the scavenger receptor CD36 is controlled by PPAR $\gamma$  (Tontonoz et al., 1998) and is involved in the uptake of A $\beta$ . To substantiate this hypothesis, primary microglia were incubated with DSP-8658 or pioglitazone for 6 h, and CD36 mRNA and protein levels were measured. CD36 mRNA was upregulated in response to DSP-8658 or pioglitazone, followed by an increase of the respective protein levels in a concentration-dependent manner (Fig. 2*C, D*). Restricting the action of CD36 by either an inhibitory antibody

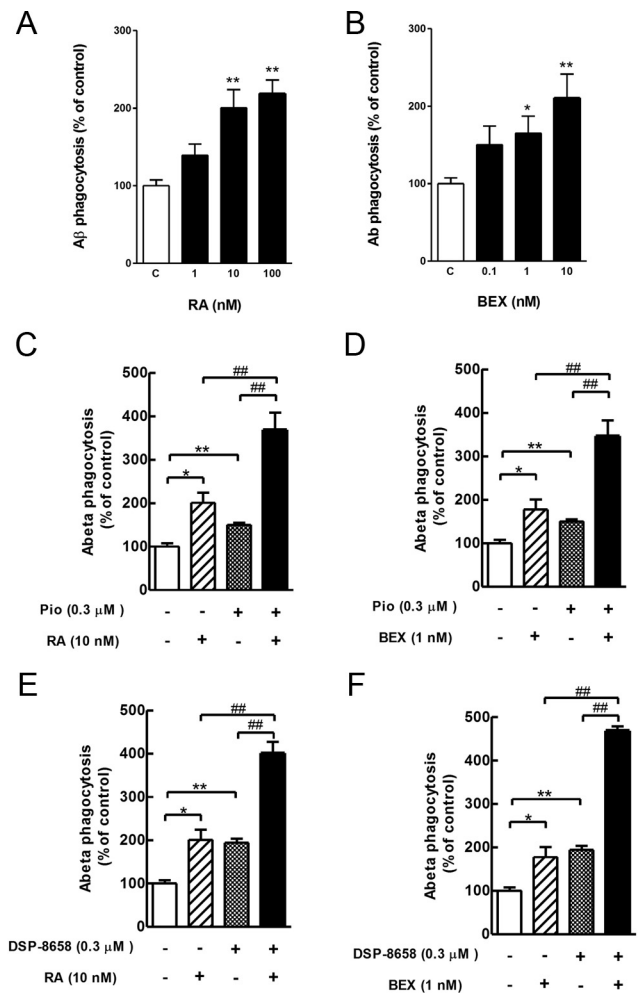


**Figure 4.** Additive effects dual activation of PPAR $\gamma$  and RXR in primary microglia. Primary microglia were incubated with indicated concentrations of retinoic acid (**A**; RA) or bexarotene (**B**; BEX) in the presence of FAM-A $\beta$  (0.5  $\mu$ M). After 4 h exposure to A $\beta$ , intracellular levels of A $\beta$  were determined. RXR agonists enhanced the uptake of A $\beta$  in rat primary microglia in a concentration-dependent manner. The data show the intracellular A $\beta$  uptake as percentage of control (mean  $\pm$  SEM of  $n = 3$ ,  $*p < 0.05$ ,  $**p < 0.01$ , one-way ANOVA, Dunnett's multiple comparison test). **C–F**, Primary microglia was incubated with the combination of pioglitazone (0.3  $\mu$ M) (**C, D**; Pio) or DSP-8658 (0.3  $\mu$ M) (**E, F**) with the RXR agonists retinoic acid (10 nM) and bexarotene (1 nM) in the presence of FAM-A $\beta$  (0.5  $\mu$ M). After 4 h exposure to A $\beta$ , intracellular levels of A $\beta$  were determined. Coincubation of PPAR $\gamma$  agonists with RXR agonists showed an additive enhancement on A $\beta$  uptake. The data show the intracellular A $\beta$  uptake as percentage of control (means  $\pm$  SEM of  $n = 3$ ,  $*p < 0.05$ ,  $**p < 0.01$  vs control,  $###p < 0.01$  vs DSP-8658, pioglitazone, retinoic acid, or bexarotene alone, one-way ANOVA, Tukey's *post hoc* test).

against CD36 or siRNA knockdown of CD36 resulted in the abolishment of the stimulatory effect of DSP-8658 or pioglitazone on A $\beta$  phagocytosis prevented the increase of A $\beta$  uptake during incubation with DSP-8658 or pioglitazone (Fig. 3). These results identify CD36 as a key mediator of PPAR $\gamma$  agonist-induced microglial A $\beta$  phagocytosis.

### Additive effects of combined activation of PPAR $\gamma$ and RXR in primary microglia

Because all PPARs heterodimerize with RXRs and subsequently bind to DNA responsive elements, thereby regulating the expression of target genes, we analyzed whether a combined activation of the PPAR $\gamma$ /RXR heterodimer would lead to an increase in A $\beta$  uptake. Two RXR agonists, retinoic acid and bexarotene, were

tested for their effect on A $\beta$  phagocytosis. Both RXR agonists enhanced A $\beta$  phagocytosis in primary microglia in a concentration-dependent manner (Fig. 4A,B). Primary microglia was then incubated with DSP-8658 or pioglitazone and the respective RXR agonists, and intracellular levels of A $\beta$  were determined after 4 h of incubation. Interestingly, the combination of pioglitazone or DSP-8658 with RXR agonists revealed an additive effect on A $\beta$  uptake (Fig. 4C–F). Because both retinoic acid and bexarotene are not isoform specific and can activate both RXR $\alpha$  and RXR $\beta$ , we determined which isoform is involved in the agonist-induced increase of A $\beta$  phagocytosis by siRNA knockdown of either RXR $\alpha$  or RXR $\beta$ . Transfection of primary rat and mouse microglia with siRNA effectively decreased RXR $\alpha$  expression (Fig. 5A,C), whereas RXR $\beta$  expression was not (rat) or only to a minor level (mouse) detected in primary microglia after transfection of both nontarget control or RXR $\beta$  siRNA. In contrast and as a positive control, RXR $\beta$  expression was found in BV2 cells (Fig. 5A), indicating that RXR $\beta$  is either not expressed or at levels below detection by Western blot. Importantly, nontarget siRNA and RXR $\beta$  siRNA did not affect the uptake of A $\beta$  in response to bexarotene (Fig. 5B,D). In contrast, suppression of RXR $\alpha$  by siRNA inhibited the bexarotene-induced increase of A $\beta$  uptake (Fig. 5B,D). These results indicated that RXR $\alpha$  represents the functionally more relevant isoform for A $\beta$  phagocytosis in primary microglia.

#### DSP-8658 treatment induced *in vivo* phagocytosis and recruitment of microglia to A $\beta$ plaques

Based on the *in vitro* data presented above and the superior ability to cross the blood–brain barrier [brain/plasma concentration ratio of 0.13:0.08 for DSP-8658/pioglitazone (Maeshiba et al., 1997)], we chose DSP-8658 for additional *in vivo* experiments. APP/PS1 transgenic mice received a DSP-8658-enriched diet from 4–6 months of age. Calculated from the monitored daily food intake, each animal received  $\sim 150 \text{ mg} \cdot \text{kg}^{-1} \cdot \text{d}^{-1}$  during treatment. So far, evaluation of *in vivo* A $\beta$  phagocytosis was conducted by immunohistochemical colocalization studies. Recently, our laboratory established a new method using the amyloid dye methoxy-X04 in combination with flow cytometrical measurement of microglial isolated directly from murine brains. For this, mice were injected with methoxy-X04 3 h before they were killed, and microglia were prepared by density gradient fractionation. Methoxy-X04-positive CD11b<sup>+</sup>/CD45<sup>+</sup> cells were detected in vehicle-treated APP/PS1 but almost absent in wild-type mice (Fig. 6A). Interestingly, DSP-8658 treatment increased the percentage of phagocytosing cells in APP/PS1 mice compared with vehicle-treated mice (Fig. 6B). We also analyzed CD36 expression

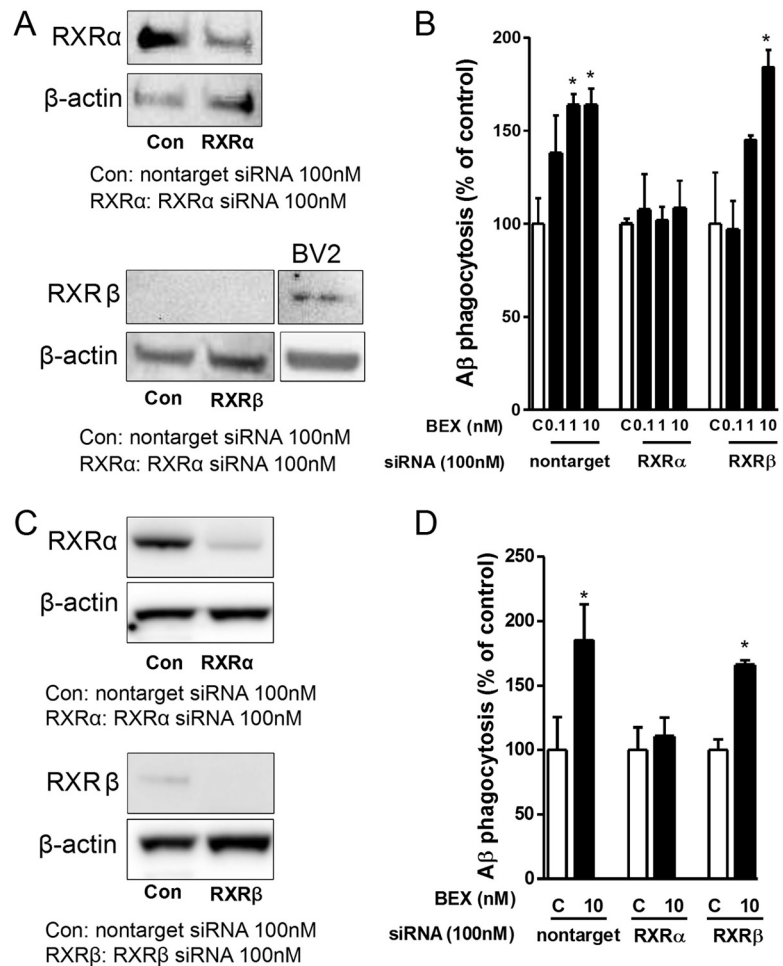


**Figure 5.** Effects of RXR $\alpha$  or RXR $\beta$  suppression on A $\beta$  phagocytosis in rat primary microglia. **A**, RXR $\alpha$  and RXR $\beta$  detection in rat primary microglia transfected with siRNA for RXR $\alpha$ , RXR $\beta$ , or nontarget. **B**, Primary microglia transfected with siRNA for RXR $\alpha$  or RXR $\beta$  were incubated with bexarotene (BEX) in the presence of FAM-A $\beta$  (0.5  $\mu\text{M}$ ). After 4 h exposure to A $\beta$ , intracellular level of A $\beta$  was determined. Phagocytosis was only suppressed by RXR $\alpha$  siRNA. The data show the intracellular A $\beta$  uptake as percentage of control (mean  $\pm$  SEM of  $n = 3$ ,  $*p < 0.05$  vs control, one-way ANOVA, Tukey's *post hoc* test). **C**, RXR $\alpha$  and RXR $\beta$  detection in murine primary microglia transfected with siRNA for RXR $\alpha$ , RXR $\beta$ , or nontarget. **D**, Primary murine microglia transfected with siRNA for RXR $\alpha$  or RXR $\beta$  were incubated with bexarotene (BEX) in the presence of FAM-A $\beta$  (0.5  $\mu\text{M}$ ). After 4 h exposure to A $\beta$ , the intracellular level of A $\beta$  was determined. Data show the intracellular A $\beta$  uptake as percentage of control (mean  $\pm$  SEM of  $n = 3$ ,  $*p < 0.05$  vs control, one-way ANOVA, Tukey's *post hoc* test).

of CD11b<sup>+</sup>/CD45<sup>+</sup>/methoxy-X04-negative (non-phagocytosing) cells and CD11b<sup>+</sup>/CD45<sup>+</sup>/methoxy-X04<sup>+</sup> (phagocytosing) cells. Although non-phagocytosing microglia did not reveal any difference in CD36 expression, DSP-8658 treatment increased CD36 expression in phagocytosing cells (Fig. 6C). To further validate this result, microglial *in vivo* phagocytosis was analyzed by confocal immunohistochemistry. We therefore analyzed the colocalization of A $\beta$  deposits with the microglial marker CD11b in 6-month-old control and DSP-8658-treated APP/PS1 mice. A $\beta$  deposits were closely surrounded by CD11b<sup>+</sup> microglia (Fig. 6D). Although the number of CD11b<sup>+</sup> microglia increased with the deposition, confocal microscopy showed that only a minority of microglial cells actually contained A $\beta$  in nontreated APP/PS1 mice (Fig. 6D–F). However, DSP-8658-treated mice revealed a 30% increase in colocalization (Fig. 6F). In addition, short-term DSP-8658 treatment for 3 d also enhanced CD36 expression *in vivo* (Fig. 6G). Interestingly, the short-term combined treatment of DSP-8658 and bexarotene for 3 d enhanced CD36 expression

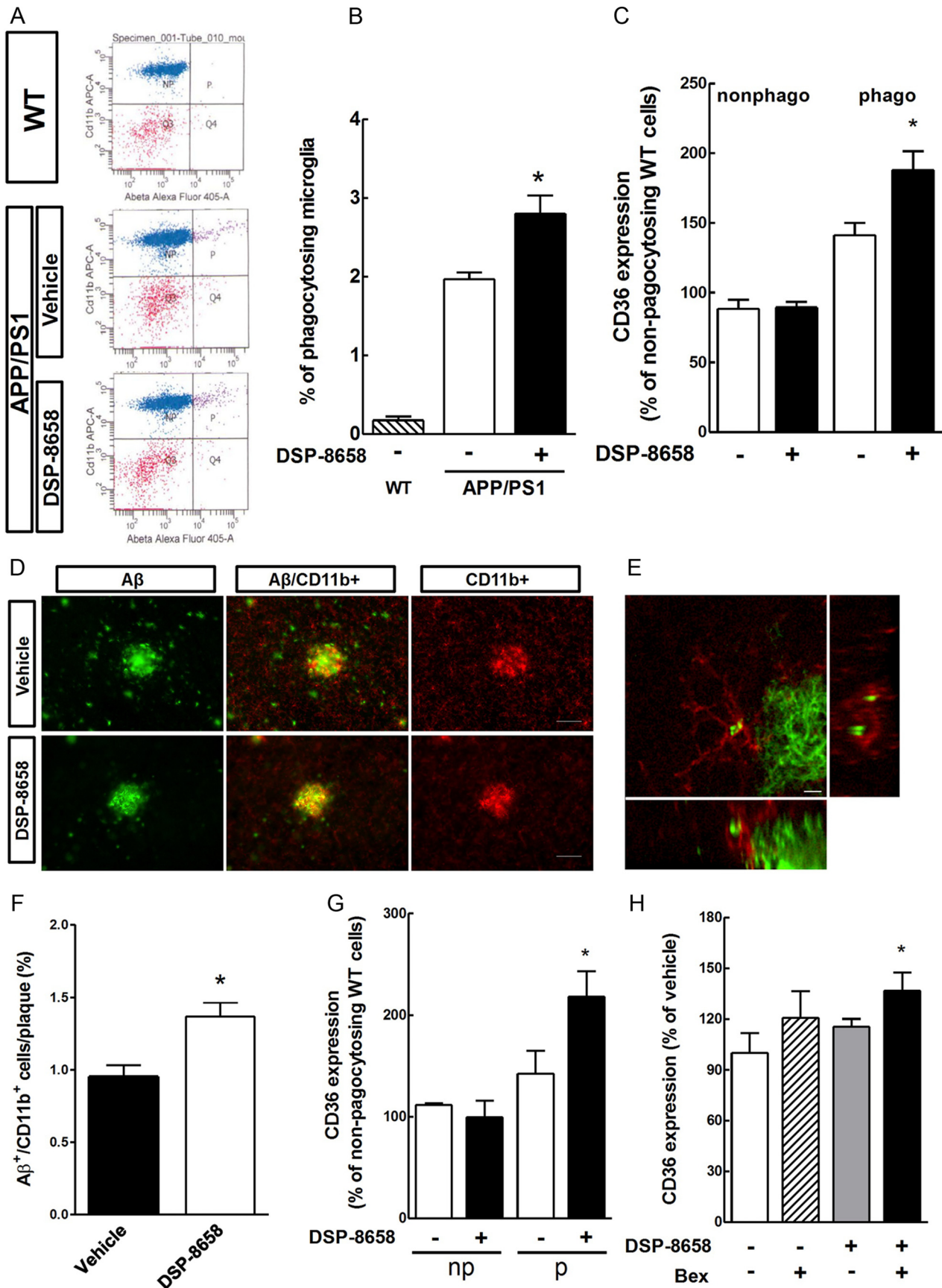


**Figure 6.** DSP-8658 induces *in vivo* A $\beta$  phagocytosis and recruitment of microglia to A $\beta$  plaques. APP/PS1 transgenic mice received either DSP-8658 or vehicle containing chow for 3 months. *A*, Scatter blots of CD11b<sup>+</sup>/CD45<sup>+</sup> isolated microglia after peripheral application of methoxy-X04. Background signal was determined using wild-type (WT) control (*Figure legend continues.*)

*in vivo* as well (Fig. 6H). These results are consistent with our *in vitro* observations and suggest that PPAR $\gamma$  agonists can be more effective in AD. In addition, the upregulated expression of CD36 may mediate the observed increase of A $\beta$  phagocytosis *in vitro* and *in vivo*.

### DSP-8658 reduces brain A $\beta$ levels

To assess whether increased phagocytosis led to an overall reduction or cerebral A $\beta$  levels, cortical and hippocampal levels of A $\beta_{1-40}$  and A $\beta_{1-42}$  were determined in APP/PS1 mice after 3 months of DSP-8658 treatment. Determination of cortex A $\beta$  levels revealed 32 and 30% decrease of both SDS-soluble A $\beta_{1-42}$  and A $\beta_{1-40}$  levels, respectively, in response to the DSP-8658 treatment (Fig. 7A). DSP-8658 treatment also decreased hippocampal SDS-soluble A $\beta_{1-42}$  levels (Fig. 7C). RIPA-soluble cortical A $\beta_{1-40}$  levels were slightly reduced by the same treatment (Fig. 7B,D). In accordance with this, A $\beta$  plaque load determined by thioflavin S staining of sagittal brain sections revealed a decrease in the cortex of DSP-8658-treated APP/PS1 mice (Fig. 7E).

### Spatial learning of DSP-8658-treated APP/PS1 transgenic mice

Because increased microglial A $\beta$  clearance from the brain may result in improved learning and memory behavior, we assessed spatial memory by the Morris water maze test. Mice were trained to escape to a submerged platform for a maximum of 40 s conducting four trials per day during 8 consecutive days. Data were analyzed with respect to average distance and latency. In DSP-8658-treated APP/PS1 mice, distance traveled and escape latency decreased gradually

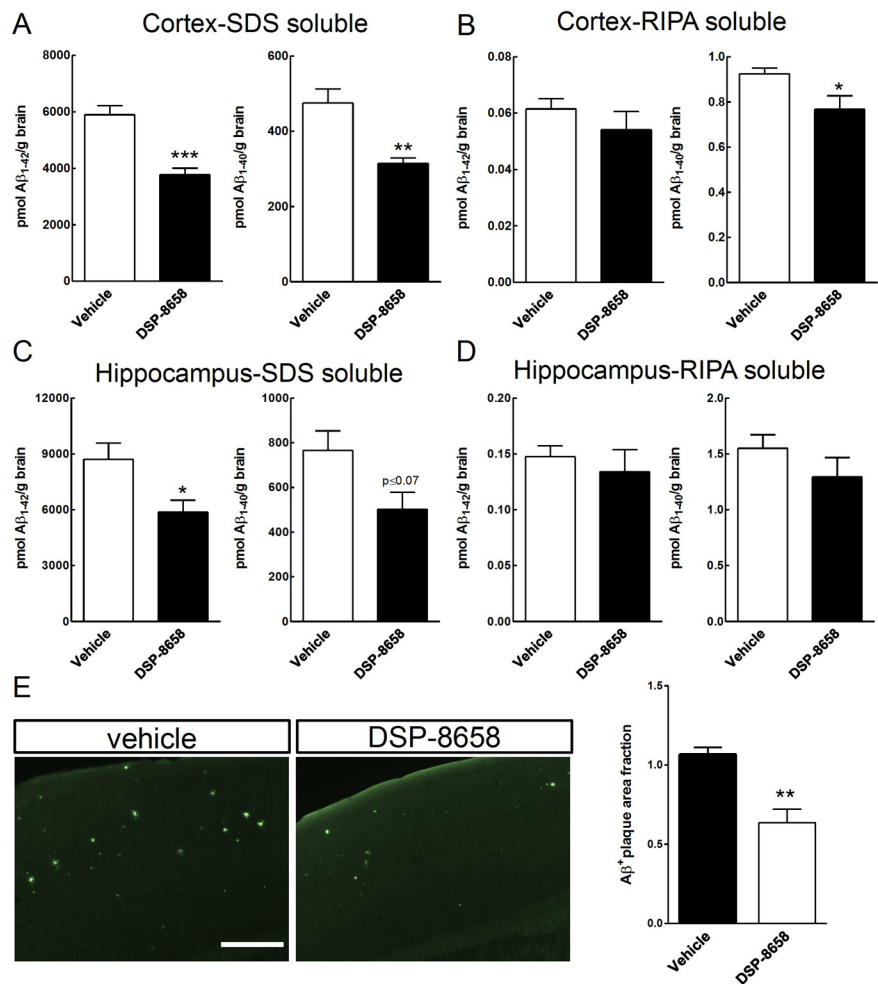


**Figure 7.** DSP-8658 reduces A $\beta$  burden in the APP/PS1 transgenic mice. APP/PS1 transgenic mice were treated with DSP-8658 in the diet for 3 months. After treatment, cortex and hippocampus were excised and protein was extracted. Concentrations of A $\beta_{1-40}$  and A $\beta_{1-42}$  in SDS-soluble (A, C) and RIPA-soluble (B, D) fractions from cortex and hippocampus of APP/PS1 mice were determined by sandwich ELISA. DSP-8658 reduced SDS-soluble A $\beta_{1-40}$  and A $\beta_{1-42}$  in cortex and SDS-soluble A $\beta_{1-42}$  in hippocampus compared with control (mean  $\pm$  SEM of  $n = 4$ , \* $p < 0.05$ , \*\* $p < 0.01$ , Student's *t* test). E, A $\beta$  deposition in the cortex was evaluated by thioflavin S staining and calculated as A $\beta$ -positive area fraction (mean  $\pm$  SEM of  $n = 4$ , \* $p < 0.05$ , Student's *t* test). Scale bar, 250  $\mu$ m.

during training. This decrease in distance and escape latency was more pronounced in DSP-8658-treated APP/PS1 mice than observed in vehicle-treated mice (Fig. 8). A quantitative analysis by calculating the area under the curve (AUC) for distance and latency verified a substantial improvement in response to DSP-8658 treatment. These results indicated that DSP-8658 ameliorated the spatial learning in AD mice.

## Discussion

Impaired cerebral A $\beta$  clearance has been proposed as the leading cause of sporadic AD, the vast majority of cases (Mawuenyega et al., 2010). One of the key functions of microglial cells in the brain is to serve as specialized sensors for brain damage. They represent the first line of defense against invading pathogens and tissue injury (Hanisch and Kettenmann, 2007; Ransohoff, 2009). On pathological stimuli, microglia become activated, migrate to and surround damaged or dead cells, and subsequently clear cellular debris from the area.

In AD, microglia can be found at the site of A $\beta$  deposition, and this assembly is thought to represent an attempt to clear the mis-

(Figure legend continued.) mice. General microglial background was determined by analysis of unstained, non-injected wild-type mice. B, The percentage of methoxy-X04<sup>+</sup>/CD11b<sup>+</sup>/CD45<sup>+</sup> cells to CD11b<sup>+</sup>/CD45<sup>+</sup> cells was calculated (mean  $\pm$  SEM of  $n = 4$ , \* $p < 0.05$ , Student's *t* test). C, FACS analysis for CD36 expression was performed in non-phagocytosing (nonphago) and phagocytosing (phago) cells (mean  $\pm$  SEM of  $n = 4$ , \* $p < 0.05$ , Student's *t* test). D, Confocal laser-scanning microscopy detected a higher number of A $\beta$ -plaque-associated and A $\beta$ -containing microglial cells in DSP-8658-treated APP/PS1 transgenic mice compared with vehicle-treated APP/PS1 controls. Scale bar, 50  $\mu$ m. E, Colocalization of A $\beta$ /Cd11b within microglia visualized by confocal laser-scanning microscopy. Scale bar, 5  $\mu$ m. F, Ten randomly chosen plaque areas were evaluated for A $\beta$ /Cd11b colocalization per animal (mean  $\pm$  SEM of  $n = 4$ , \* $p < 0.05$ , Student's *t* test). G, APP/PS1 transgenic mice were treated with DSP-8658 for 3 d and injected with methoxy-X04 3 h before analysis. After isolation of microglia, CD36 expression was determined by flow cytometry in non-phagocytosing (np) and phagocytosing (p) cells. Values were normalized to the CD36 expression in untreated microglia from age-matched wild-type mice (mean  $\pm$  SEM of  $n = 4$ , \* $p < 0.05$ , Student's *t* test). H, APP/PS1 transgenic mice were treated with DSP-8658 or bexarotene (Bex) and the combination of these compounds for 3 d. Isolated phagocytosing microglia were analyzed by FACS for CD36 expression per animal (mean  $\pm$  SEM of  $n = 4$ , \* $p < 0.05$ , Student's *t* test).



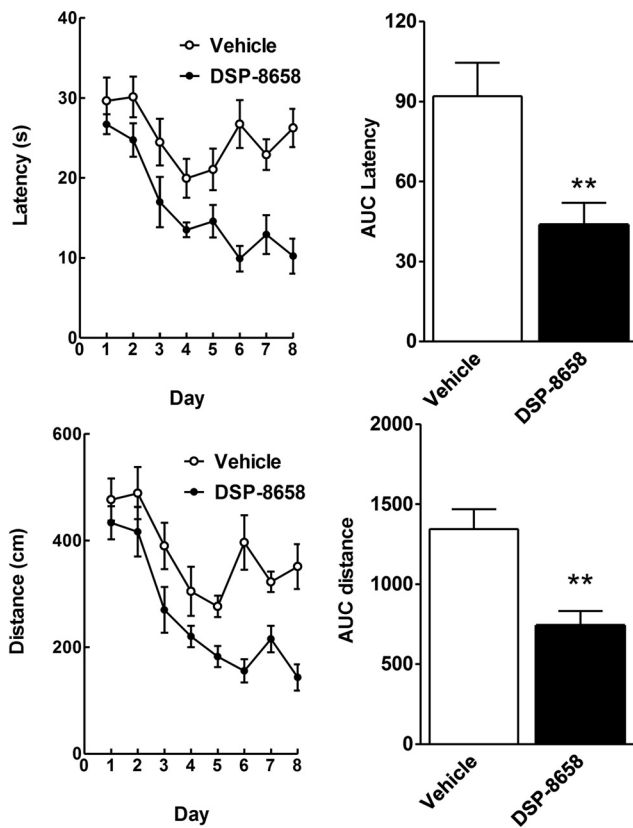


**Figure 8.** DSP-8658 treatment improved spatial memory learning of APP/PS1 transgenic mice. APP/PS1 transgenic mice were treated with DSP-8658 for 3 months. After treatment, all animals were subjected to the Morris water maze test. The time needed to reach the hidden platform (latency, seconds) and distance traveled (distance, centimeters) are depicted over 8 consecutive days. Integrated time and distance traveled (AUC) were determined for the whole observation period. Data represent means  $\pm$  SEM ( $n = 9$  for vehicle and  $n = 10$  for DSP-8658,  $**p < 0.01$ , Student's  $t$  test).

folded and aggregated A $\beta$  peptides from the brain. A $\beta$  itself, however, results in a heterogeneous activation of microglia, including cells that develop a phagocytic phenotype (M1 state or classical activation) and release a variety of pro-inflammatory cytokines and chemokines but also cells that convert to an alternative activation state (M2 state) induced by anti-inflammatory cytokines and chemokines, which is thought to contribute to tissue repair and regeneration (Town et al., 2005; Colton et al., 2006).

However, persisting neuroinflammation and sustained exposure to proinflammatory stimuli compromises microglial clearance functions as AD progresses (Lee and Landreth, 2010). In turn, suppression of inflammation can restore A $\beta$  phagocytosis (Heneka et al., 2010b). There are also indications that inhibition of anti-inflammatory stimuli has beneficial effects on A $\beta$  phagocytosis,  $\beta$ -amyloidosis, and cognitive function (Town et al., 2008).

Activation of PPAR $\gamma$  by endogenous or synthetic ligands modulates insulin sensitivity and exerts profound anti-inflammatory effects in peripheral macrophages and microglia. Less is known, however, about the functional consequences of microglial PPAR $\gamma$  activation under inflammatory stimulation. We hypothesized that the anti-inflammatory action of PPAR $\gamma$  activation would improve microglial clearance function. Currently marketed PPAR $\gamma$  ligands, such as rosiglitazone or pioglitazone, only show a minor blood–brain barrier penetra-

tion. They also carry a number of undesirable side effects. Therefore, novel drugs, such as DSP-8658, which acts as a dual PPAR $\alpha$ / $\gamma$  modulator, are currently under clinical development for the treatment of type 2 diabetes and AD. In this study, we investigated the mechanisms and potential of pioglitazone and DSP-8658 to positively modulate microglial A $\beta$  phagocytosis.

Both substances DSP-8658 and pioglitazone enhanced A $\beta$  phagocytosis in primary microglia without affecting its degradation. Because several synthetic PPAR $\gamma$  ligands execute “off-target” actions, we tested the specificity of the observed effects under PPAR $\gamma$  knockdown conditions. Using primary microglia transfected with PPAR $\gamma$  siRNA, we found that neither pioglitazone nor DSP-8658 were able to increase A $\beta$  phagocytosis, thus confirming PPAR $\gamma$  dependency. Of note, this effect was abolished by coincubation with transcriptional or translational inhibitors, suggesting that the observed effect requires *de novo* protein synthesis.

CD36 is a pivotal target of PPAR $\gamma$ -mediated gene regulation in macrophages and has also been suggested as important receptor for microglial A $\beta$  phagocytosis (Coraci et al., 2002; Zhao et al., 2009). In addition, it mediates the innate immune response caused by fibrillar A $\beta$ , resulting in the proinflammatory secretion of cytokines, chemokines, and reactive oxygen species (El Khoury et al., 2003). Thus, microglia interacts with A $\beta$  through a recently characterized cell-surface receptor complex comprising CD36,  $\alpha 6 \beta 1$  integrin, and CD47 (Lee and Landreth, 2010). Therefore we tested whether exposure of cells to pioglitazone or DSP-8658 would result in a functionally relevant CD36 expression. DSP-8658 and pioglitazone enhanced CD36 mRNA and protein levels in primary microglia. Importantly, PPAR $\gamma$  agonist-stimulated A $\beta$  phagocytosis was abolished by coincubation of inhibitory CD36 antibody or likewise by transfection of cells with CD36 siRNA. These results indicate clearly that PPAR $\gamma$  agonist-induced upregulation of CD36 promotes microglia-mediated phagocytosis.

PPAR $\gamma$  heterodimerizes with RXRs (Tugwood et al., 1992), and, during ligand activation, the PPAR/RXR heterodimer recruits coactivators and binds to sequence-specific PPAR response elements present in the promoter region of several target genes. Recently, the RXR agonist bexarotene has been reported to facilitate the intracellular degradation of soluble A $\beta_{1-42}$  in a PPAR $\gamma$ -, liver X receptor-, and apolipoprotein E-dependent manner (Cramer et al., 2012). Here we show that two structurally different RXR agonists, bexarotene and retinoic acid, increase microglial A $\beta$  phagocytosis. Dual activation of both heterodimer partners has been reported previously to show increased efficacy compared with the activation of a single heterodimer partner (Papi et al., 2009). Likewise, the combination of DSP-8658 and pioglitazone with RXR agonists (retinoic acid and bexarotene) showed an additive enhancement of A $\beta$  uptake in the present study. Using siRNA-based knockdown analysis for RXR $\alpha$  or RXR $\beta$ , we revealed that RXR $\alpha$  represents the functionally important RXR in primary microglia. Therefore, we suggest that a combination therapy using agonists of PPAR $\gamma$  and RXR $\alpha$  may be more effective in AD.

Several studies analyzed the effect of pioglitazone treatment in animal models of AD. An acute treatment of 10-month-old APPV717I mice with pioglitazone or ibuprofen reduced the number of activated microglia, reactive astrocytes, and overall A $\beta$  deposition in the hippocampus and frontal cortex (Heneka et al., 2005). Yan et al., 2003 found that 6-month treatment of Tg2576 mice with pioglitazone resulted

in a modest reduction in soluble A $\beta$  levels with no effect on plaque burden or inflammation. The absence of a substantial effect was postulated to be attributable to poor penetration of pioglitazone into the brain (Maeshiba et al., 1997). DSP-8658 passes the blood–brain barrier more effectively than pioglitazone (data not shown). Therefore, verification of the above described *in vitro* findings was performed using DSP-8658 in APP/PS1 transgenic mice. Using the amyloid dye methoxy-X04 in combination with flow cytometrical measurement of microglial isolated from brains of adult DSP-8658-treated and untreated mice, we found that DSP-8658 treatment increased the percentage of phagocytosing cells in APP/PS1 mice, confirming our *in vitro* observations. Moreover, these data were further supported by confocal microscopy showing that only a minority of microglia contained A $\beta$  in nontreated APP/PS1 mice, while DSP-8658-treated mice revealed a 30% increase in colocalization. DSP-8658 finally reduced cortical and hippocampal SDS-soluble A $\beta_{1-42}$  and A $\beta_{1-40}$  levels and decreased A $\beta$  plaque load. Increase in phagocytosis and subsequently reduced levels of A $\beta$  were accompanied by a substantial improvement of spatial memory performance.

In summary, PPAR $\gamma$  activation by DSP-8658 or pioglitazone alone or, more effectively, in combination with RXR $\alpha$  activation, enhances microglial A $\beta$  phagocytosis by upregulation of CD36. Moreover, we revealed that DSP-8658 treatment increased microglial A $\beta$  phagocytosis *in vivo*, resulting in an overall reduction of A $\beta$  levels and improved spatial memory performance. Based on these results, PPAR $\gamma$ /RXR activators that efficiently cross the blood–brain barrier may be considered as future therapeutics for AD.

## References

- Bamberger ME, Harris ME, McDonald DR, Husemann J, Landreth GE (2003) A cell surface receptor complex for fibrillar  $\beta$ -amyloid mediates microglial activation. *J Neurosci* 23:2665–2674. [Medline](#)
- Bolmont T, Haiss F, Eicke D, Radde R, Mathis CA, Klunk WE, Kohsaka S, Jucker M, Calhoun ME (2008) Dynamics of the microglial/amyloid interaction indicate a role in plaque maintenance. *J Neurosci* 28:4283–4292. [CrossRef Medline](#)
- Colton CA, Mott RT, Sharpe H, Xu Q, Van Nostrand WE, Vitek MP (2006) Expression profiles for macrophage alternative activation genes in AD and in mouse models of AD. *J Neuroinflammation* 3:27. [CrossRef Medline](#)
- Combs CK, Johnson DE, Karlo JC, Cannady SB, Landreth GE (2000) Inflammatory mechanisms in Alzheimer's disease: inhibition of beta-amyloid-stimulated proinflammatory responses and neurotoxicity by PPAR $\gamma$  agonists. *J Neurosci* 20:558–567. [Medline](#)
- Coraci IS, Husemann J, Berman JW, Hulette C, Dufour JH, Campanella GK, Luster AD, Silverstein SC, El-Khoury JB (2002) CD36, a class B scavenger receptor, is expressed on microglia in Alzheimer's disease brains and can mediate production of reactive oxygen species in response to beta-amyloid fibrils. *Am J Pathol* 160:101–112. [CrossRef Medline](#)
- Cramer PE, Cirrito JR, Wesson DW, Lee CY, Karlo JC, Zinn AE, Casali BT, Restivo JL, Goebel WD, James MJ, Brunden KR, Wilson DA, Landreth GE (2012) ApoE-directed therapeutics rapidly clear  $\beta$ -amyloid and reverse deficits in AD mouse models. *Science* 335:1503–1506. [CrossRef Medline](#)
- El Khoury JB, Moore KJ, Means TK, Leung J, Terada K, Toft M, Freeman MW, Luster AD (2003) CD36 mediates the innate host response to beta-amyloid. *J Exp Med* 197:1657–1666. [CrossRef Medline](#)
- El Khoury J, Toft M, Hickman SE, Means TK, Terada K, Geula C, Luster AD (2007) Ccr2 deficiency impairs microglial accumulation and accelerates progression of Alzheimer-like disease. *Nat Med* 13:432–438. [CrossRef Medline](#)
- Fleisher-Berkovich S, Filipovich-Rimon T, Ben-Shmuel S, Hülsmann C, Kummer MP, Heneka MT (2010) Distinct modulation of microglial amyloid  $\beta$  phagocytosis and migration by neuropeptides (i). *J Neuroinflammation* 7:61. [CrossRef Medline](#)
- Floden AM, Combs CK (2006)  $\beta$ -Amyloid stimulates murine postnatal and adult microglia cultures in a unique manner. *J Neurosci* 26:4644–4648. [CrossRef Medline](#)
- Hanisch UK, Kettenmann H (2007) Microglia: active sensor and versatile effector cells in the normal and pathologic brain. *Nat Neurosci* 10:1387–1394. [CrossRef Medline](#)
- Heneka MT, Landreth GE (2007) PPARs in the brain. *Biochim Biophys Acta* 1771:1031–1045. [CrossRef Medline](#)
- Heneka MT, Feinstein DL, Galea E, Gleichmann M, Wüllner U, Klockgether T (1999) Peroxisome proliferator-activated receptor gamma agonists protect cerebellar granule cells from cytokine-induced apoptotic cell death by inhibition of inducible nitric oxide synthase. *J Neuroimmunol* 100:156–168. [CrossRef Medline](#)
- Heneka MT, Sastre M, Dumitrescu-Ozimek L, Hanke A, Dewachter I, Kuiperi C, O'Banion K, Klockgether T, Van Leuven F, Landreth GE (2005) Acute treatment with the PPARgamma agonist pioglitazone and ibuprofen reduces glial inflammation and Abeta1–42 levels in APPV717I transgenic mice. *Brain* 128:1442–1453. [CrossRef Medline](#)
- Heneka MT, Nadrigny F, Regen T, Martinez-Hernandez A, Dumitrescu-Ozimek L, Terwel D, Jardanhazi-Kurutz D, Walter J, Kirchhoff F, Hanisch UK, Kummer MP (2010a) Locus ceruleus controls Alzheimer's disease pathology by modulating microglial functions through norepinephrine. *Proc Natl Acad Sci U S A* 107:6058–6063. [CrossRef Medline](#)
- Heneka MT, O'Banion MK, Terwel D, Kummer MP (2010b) Neuroinflammatory processes in Alzheimer's disease. *J Neural Transm* 117:919–947. [CrossRef Medline](#)
- Hickman SE, Allison EK, El Khoury J (2008) Microglial dysfunction and defective  $\beta$ -amyloid clearance pathways in aging Alzheimer's disease mice. *J Neurosci* 28:8354–8360. [CrossRef Medline](#)
- in 't Veld BA, Ruitenbergh A, Hofman A, Launer LJ, van Duijn CM, Stijnen T, Breteler MM, Stricker BH (2001) Nonsteroidal antiinflammatory drugs and the risk of Alzheimer's disease. *N Engl J Med* 345:1515–1521. [CrossRef Medline](#)
- Jäger S, Leuchtenberger S, Martin A, Czirr E, Wesselowski J, Dieckmann M, Waldron E, Korth C, Koo EH, Heneka M, Weggen S, Pietrzik CU (2009) alpha-secretase mediated conversion of the Amyloid Precursor Protein derived membrane stub C99 to C83 limits Abeta generation. *J Neurochem* 111:1369–1382. [CrossRef Medline](#)
- Jankowsky JL, Slunt HH, Ratovitski T, Jenkins NA, Copeland NG, Borchelt DR (2001) Co-expression of multiple transgenes in mouse CNS: a comparison of strategies. *Biomol Eng* 17:157–165. [CrossRef Medline](#)
- Jiang C, Ting AT, Seed B (1998) PPAR-gamma agonists inhibit production of monocyte inflammatory cytokines. *Nature* 391:82–86. [CrossRef Medline](#)
- Lee CY, Landreth GE (2010) The role of microglia in amyloid clearance from the AD brain. *J Neural Transm* 117:949–960. [CrossRef Medline](#)
- Lehmann JM, Lenhard JM, Oliver BB, Ringold GM, Kliewer SA (1997) Peroxisome proliferator-activated receptors alpha and gamma are activated by indomethacin and other non-steroidal anti-inflammatory drugs. *J Biol Chem* 272:3406–3410. [CrossRef Medline](#)
- Lucin KM, Wyss-Coray T (2009) Immune activation in brain aging and neurodegeneration: too much or too little? *Neuron* 64:110–122. [CrossRef Medline](#)
- Maeshiba Y, Kiyota Y, Yamashita K, Yoshimura Y, Motohashi M, Tanayama S (1997) Disposition of the new antidiabetic agent pioglitazone in rats, dogs, and monkeys. *Arzneimittelforschung* 47:29–35. [Medline](#)
- Mawuenyega KG, Sigurdson W, Ovod V, Munsell L, Kasten T, Morris JC, Yarasheski KE, Bateman RJ (2010) Decreased clearance of CNS beta-amyloid in Alzheimer's disease. *Science* 330:1774. [CrossRef Medline](#)
- McGeer PL, Schulzer M, McGeer EG (1996) Arthritis and anti-inflammatory agents as possible protective factors for Alzheimer's disease: a review of 17 epidemiologic studies. *Neurology* 47:425–432. [CrossRef Medline](#)
- Papi A, Tatenhorst L, Terwel D, Hermes M, Kummer MP, Orlandi M, Heneka MT (2009) PPARgamma and RXRgamma ligands act synergistically as potent antineoplastic agents in vitro and in vivo glioma models. *J Neurochem* 109:1779–1790. [CrossRef Medline](#)
- Ransohoff RM (2009) Chemokines and chemokine receptors: standing at the crossroads of immunobiology and neurobiology. *Immunity* 31:711–721. [CrossRef Medline](#)
- Ricote M, Li AC, Willson TM, Kelly CJ, Glass CK (1998) The peroxisome proliferator-activated receptor-gamma is a negative regulator of macrophage activation. *Nature* 391:79–82. [CrossRef Medline](#)

- Rogers J, Lue LF (2001) Microglial chemotaxis, activation, and phagocytosis of amyloid beta-peptide as linked phenomena in Alzheimer's disease. *Neurochem Int* 39:333–340. [CrossRef Medline](#)
- Stewart WF, Kawas C, Corrada M, Metter EJ (1997) Risk of Alzheimer's disease and duration of NSAID use. *Neurology* 48:626–632. [CrossRef Medline](#)
- Terwel D, Steffensen KR, Verghese PB, Kummer MP, Gustafsson JÅ, Holtzman DM, Heneka MT (2011) Critical role of astroglial apolipoprotein E and liver X receptor- $\alpha$  expression for microglial A $\beta$  phagocytosis. *J Neurosci* 31:7049–7059. [CrossRef Medline](#)
- Tontonoz P, Nagy L, Alvarez JG, Thomazy VA, Evans RM (1998) PPAR- $\gamma$  promotes monocyte/macrophage differentiation and uptake of oxidized LDL. *Cell* 93:241–252. [CrossRef Medline](#)
- Town T, Nikolic V, Tan J (2005) The microglial "activation" continuum: from innate to adaptive responses. *J Neuroinflammation* 2:24. [CrossRef Medline](#)
- Town T, Laouar Y, Pittenger C, Mori T, Szekeley CA, Tan J, Duman RS, Flavell RA (2008) Blocking TGF- $\beta$ -Smad2/3 innate immune signaling mitigates Alzheimer-like pathology. *Nat Med* 14:681–687. [CrossRef Medline](#)
- Tugwood JD, Issemann I, Anderson RG, Bundell KR, McPheat WL, Green S (1992) The mouse peroxisome proliferator activated receptor recognizes a response element in the 5' flanking sequence of the rat acyl CoA oxidase gene. *EMBO J* 11:433–439. [Medline](#)
- Yan Q, Zhang J, Liu H, Babu-Khan S, Vassar R, Biere AL, Citron M, Landreth G (2003) Anti-inflammatory drug therapy alters  $\beta$ -amyloid processing and deposition in an animal model of Alzheimer's disease. *J Neurosci* 23:7504–7509. [Medline](#)
- Zhao X, Grotta J, Gonzales N, Aronowski J (2009) Hematoma resolution as a therapeutic target: the role of microglia/macrophages. *Stroke* 40:S92–S94. [CrossRef Medline](#)